Engineering Elastin-like Polypeptide-Poly(ethylene glycol) Multiblock Physical Networks

Andreia Araújo [1], Bradley D. Olsen [2], Ana Vera Machado [1*]

[1] Institute for Polymers and Composites/I3N, University of Minho, Campus de Azurém 4800-058 Guimarães, Portugal, andreiaaraujo@dep.uminho.pt; avm@dep.uminho.pt

[2] Department of Chemical Engineering, Massachusetts Institute of Technology, Cambridge, Massachusetts 02139, United States, bdolsen@mit.edu

Abstract

Hybrids of protein biopolymers and synthetic polymers are a promising new class of soft materials, as the advantages of each component can be complementary. A recombinant elastinlike polypeptide (ELP) was conjugated to poly(ethylene glycol) (PEG) by macromolecular coupling in solution to form multi-block ELP-PEG copolymers. The hydrated copolymer preserved the thermoresponsive properties from the ELP block and formed hydrogels with different transition temperatures depending on salt concentration. Small angle scattering indicates that the copolymer hydrogels form sphere-like aggregates with a "fuzzy" interface, while the films form a fractal network of nanoscale aggregates. The use of solutions with different salt concentrations to prepare the hydrogels was found to influence the transition temperature, the mechanical properties, and the size of the nanoscale structure of the hydrogel without changing the secondary structure of the ELP. The salt variation and the addition of a plasticizer also affected the nanoscale structure and the mechanical characteristics of the films.

KEYWORDS

PEG, ELP, physical networks, hydrogel, thin film

INTRODUCTION

Nature has repeatedly surpassed engineers when designing functional materials that are capable of withstanding complex and harsh environmental conditions while maintaining their superior mechanical properties [1]. Bone, collagen and spider silk are examples of hierarchical structures that, under deformation or stress, utilize multiple levels of

organization to absorb energy and reinforce the material [2]. Efforts to mimic Nature's structures and functions in the design of new materials and active assemblies have encouraged engineers to look to proteins as a source of building blocks for the next generation of polymeric materials [3–4]. A few examples are bioinspired polymers [5] and synthetic enzymes [6] that use traditional polymer materials to mimic the performance of proteins, protein-polymer hybrids that incorporate both types of molecules into a single material [7], and artificially engineered protein-polymers that apply the design principles of polymer science to the engineering of new proteins [3,8].

Proteins are polyamides composed of a combination of 20 different amino acids in linear chains. They comprise one of the most impressive categories of polymers known [9] : they produce high-performance fibers [10], extremely strong and tough materials [11] and underwater adhesives [12], harvest light by converting it into chemical energy [13], efficiently catalyze chemical transformations [14] and selectively bind analytes in complex mixtures [15].

Elastin-like polypeptides (ELPs) [16] are one of the most commonly studied protein materials; these engineered biopolymers capture many of the features of natural elastin in a short amino acid repeat. Natural elastin is an enzymatically crosslinked form of the tropoelastin monomer, a natural component of the extracellular matrix (ECM) found in lungs, skin, and blood vessels [17]. ELP polypeptides consist of many repeats and variations of the canonical pentapeptide VPGXG [18]. They exhibit a lower critical solution temperature (LCST), becoming insoluble in water when heated above their transition temperature. ELPs represent a promising class of biomaterials that may be formulated as gels, films, nanofibers or micelles with potential applications in drug delivery, tissue engineering or as components of implanted medical devices [19].

ELPs have been chemically synthesized and genetically engineered, particularly by varying sequence and chain length, in order to tune its physical and functional properties, including transition temperature and mechanical stiffness [20–21]. Crosslinking of ELPs through chemical, radiation or enzymatic processes have also been used for additional manipulation of physical properties [20,22]. Another way of changing the material characteristics is the production of ELP triblock copolymers with an ABA structure, with a central hydrophilic B -block and a hydrophobic and cross-linkable A-block at the ends [23–24].

Hybrids of protein biopolymers and synthetic polymers provide a promising alternative for the design of ELP networks, as the advantages of each component can be complementary. Peptides and proteins self-assemble into the native structures encoded by their primary sequence to support a diverse and complex array of functions [25]. They provide hierarchical self-assembly over multiple length scales down to the molecular level, chemical functionality, selectivity and specificity, and dynamic responses to external stimuli. Polymers are well-known for their stability, processability and versatility, as they can be water- or oil- soluble, stimuli-responsive, brittle, elastomeric, conductive, and much more [26–28]. Elastin-like sequences have been coupled to synthetic polymers, creating hybrid materials that maintained LCST behaviour [24,29]. Polyethylene glycol (PEG) has been commonly used as a polymeric conjugation partner for proteins, mainly in the form of AB-type and ABA-type triblock copolymers [29–30]. However, to our knowledge, there have only been a few studies of alternating $(AB)_m$-type multiblock copolymers commonly found in polymer networks with control over sites of conjugation between peptides and PEGs, and the highest molecular

weight obtained for PEG/elastin-mimetic hybrid polymers was around 30 and 50kDa[31–35].

Therefore, the present study aims to integrate the structural and functional properties of ELPs with the versatility of synthetic polymers, creating linear alternating block copolymers with higher molecular weight that are capable of network or gel formation due to aggregation of the ELP blocks. A recombinant ELP with size of 26 kDa was first expressed and purified, then reacted with a 20 kDa PEG by macromolecular coupling in solution. The resulting materials formed physical networks, with the advantage of not using crosslinking agents, that were characterized and processed in the form of hydrogels and films, suitable for biomedical application. The influence of salt and the addition of a plasticizer on its structure and mechanical properties were evaluated.

EXPERIMENTAL

Protein Expression and Purification

The ELP sequence explored in this work is generalized as $([I^{0.6}\ V^{0.4}]PAVG)_{50}$ and has been previously identified in the literature as "plastic" ELP, based on its apparent mechanical response in the bulk state due to the presence of alanine in the canonical pentapeptide repeat. The sequence used here, containing a specific Valine-Isoleucine ratio, is reported to reversibly form extremely stiff, nanoscale networks from solution due to kinetically arrested phase separation [36]. The ELP sequence used was modified by the addition of sequences encoding biofunctional RGD groups and cysteine residues for macromolecular coupling, yielding an encoded protein sequence shown in Fig. 1a. These modifications were introduced onto the N - and C - termini of the ELP using a one-step ligation strategy in pETA plasmids, as previously reported by Glassman et. al. [37]. Telechelic ELPs with flanking sequences containing cysteine and cell adhesive sites were expressed in Tuner(DE3) cells, typically using 5 mL overnight cultures to inoculate 1 L expressions in Terrific Broth under kanamycin selection, and expression was induced with 0.5 mM IPTG at an $OD_{600} = 0.9 - 1.1$. Cells were harvested by centrifugation 6 h postinduction, and cell pellets were resuspended in non-denaturing lysis buffer (MENT buffer: $5mMMgCl_2$, 1mM EDTA, 100 mM NaCl, 10 mM Tris, $pH = 7.5$) at a concentration of approximately 30 g wet cell mass (WCM) per 100 mL buffer. Lysozyme (100 mg per 100 mL resuspension) was added for approximately 1 h , after which the suspension was sonicated. Cell debris was removed by centrifugation, and RNAse A and DNAse I were added to the clarified supernatant (2 – 4mg per 100 mL cell suspension). The suspension was incubated at 37°C for at least 2 hours. Then, the proteins were isolated by three rounds of thermal precipitation in buffer, cycling between 4 °C and 37°C, dialyzed against water and lyophilized. The yield of ELP was ~ 100mg/L culture, and purity was confirmed by denatured state polyacrylamide gel electrophoresis (SDS-PAGE).

Conjugation

Thiol-maleimide conjugations were prepared in sodium phosphate buffer (50mM, pH = 7.4). This Michael addition reaction proceeds without metal catalysts to high conversion and has been extensively utilized for bioconjugations [38]. Lyophilized protein (20wt%) was dissolved overnight at 4 °C. Tris(2-carboxyethylphosphine) (TCEP), dissolved in the

buffer immediately prior to use, and added stoichiometrically to the thiol. PEG-bismaleimide 20 kDa (from Creative PEGWorks) was dissolved in buffer and added to the protein solution to achieve an equimolar quantity of cysteine residues and maleimide groups. The reaction was allowed to proceed overnight at $4\,^{\circ}\mathrm{C}$ under constant stirring. Conjugates were dialyzed against ultrapure water under conditions where both protein and polymer were retained, and the final product was lyophilized.

Preparation of Hydrogels

Thermoresponsive hydrogels were prepared at 15wt% by first dissolving the lyophilized bioconjugate in ultrapure water or buffer (sodium phosphate buffer at either 50 mM or 100 mM , $\mathrm{pH} = 7.6$) on ice for several hours, until a clear, viscous liquid was obtained. The samples were then heated to room temperature (RT) to form the hydrogel via a thermoresponsive structural transition.

Preparation of thin films

Thin films were produced by dissolving lyophilized bioconjugate at 9wt% in ultrapure water or sodium phosphate buffer $50\mathrm{mM}, \mathrm{pH} = 7.6$ on ice overnight. To reduce the brittleness and improve processability of protein-based materials, addition of plasticizers is generally required. Therefore, after complete dissolution, poly(ethylene glycol) dimethyl ether ($\mathrm{Mn} = 250\ \mathrm{g/mol}$) was added at 5%(v/v) to act as a plasticizer (P). Samples of $300\mu\,\mathrm{L}$ were placed on poly(tetrafluoroethylene) (PTFE) sheets and dried at 35% relative humidity (RH) and room temperature for 48 hours to obtain thin films.

Thermal analysis

Differential scanning calorimetry (DSC) analysis was performed in a Perkin-Elmer DSC 7 under nitrogen. Approximately 6 mg of each sample (powder, lyophilized, hydrogel and film) was cut and placed in an aluminum pan. Two heating ramps were run at $1^{\circ}\mathrm{C/min}$, from $0 - 37\ ^{\circ}\mathrm{C}$ for hydrogels, for films from $0 - 100\,^{\circ}\mathrm{C}$ at $10\,^{\circ}\mathrm{C/min}$ and for powder and lyophilized material at $10\,^{\circ}\mathrm{C/min}$ from $0 - 140^{\circ}\mathrm{C}$, with a 20 minutes waiting time between cycles. The results were collected from the second cycle, except for the lyophilized material where the first heating cycle was presented. The degree of crystallinity, χ_c, was calculated from the second cycle using the following formula:

$$\chi_c = \frac{\Delta H_m}{\Delta H_m^0} \times 100 \qquad (eq.\,1)$$

where ΔH_m^0 is the heat of melting of 100% crystalline polymer (196.8 J/g for PEG[39]) and ΔH_m is the heat of melting for the polymer under investigation.

Thermogravimetric analysis (TGA) was performed using a TGA Q500 (TA Instruments) under nitrogen. Around 10 mg of PEG powder, lyophilized protein and bioconjugate were run at $10\,^{\circ}\mathrm{C}$ /min from $40 - 600^{\circ}\mathrm{C}$.

Rheology

Linear oscillatory shear rheology measurements were conducted on an Anton Paar MCR-301 stress controlled rheometer in Direct Strain Oscillation mode for pseudo-strain control. The rheometer was outfitted with a Peltier heating system with an environmental enclosure for uniform temperature control. Bioconjugate hydrogels (15wt%) were loaded at 0 °C into a sandblasted cone-and-plate geometry using a 25 mm, 1° cone where the gap was zeroed at 37°C and corrected for thermal expansion. A mineral oil barrier was used to prevent sample dehydration. Frequency sweeps were acquired from 0.01 to 100rad/s at 37°C and 1% strain. To determine the gel point of ELP/PEG, the storage (G') and loss modulus (G'') were measured as a function of increasing temperature from 0 to 37°C at a rate of 1 °C/min, ω = 100rad/s and 1% strain. Gelation temperature was defined as the temperature at which G' equals G' [40].

Dynamic Mechanical Analysis

Dynamic mechanical analysis (DMA) measurements were made on rectangular film samples with dimensions 8.0 × 2.0 × 0.08 mm using a Triton Technology DMA. Samples were evaluated in tension using a dynamic temperature sweep to measure the storage and loss moduli (E ' and E '') as a function of temperature at a fixed frequency (1 Hz). The specimen's temperature was equilibrated at 25°C followed by a constant heating rate of 5°C/min to 100°C.

Fourier Transformed Infrared Spectroscopy

Room temperature infrared spectra (FTIR) of the lyophilized protein and bioconjugate, PEG powder and bioconjugate films were recorded on a Jasco spectrometer using attenuated total reflectance (ATR) mode in the range $4000 - 600\ cm^{-1}$, at room temperature, by averaging 64 scans and using a resolution of $8\ cm^{-1}$.

Following the procedure published in the literature [41], the analysis of the secondary structure was determined from the shape of the Amide I band, located around 1700 and $1600\ cm^{-1}$, using the program OriginPro v9.0. The following steps were performed: baseline correction, normalization, second derivative and iterative curve fitting using Gaussian functions ($R^2 > 0.995$). For all the characterizations was used a second derivative with a nine-point SavitskyGolay function. The peaks detected by the second derivative were used for peak position guidance during the iterative curve fitting and the area of each individual band was used to evaluate the relative contribution to the proteins' secondary structure.

Raman spectroscopy

Room temperature Raman spectra were recorded in a LabRAM HR Evolution spectrometer equipped with a 532 nm laser (Laser Quantum Torus 532, power 50 to 750 mW). The Raman spectra of the samples were acquired in the range $600 - 3500\ cm - 1$ (acquisition time: 60 s ; accumulations: 60 ; RTD time: 40 ; grating: 600gr/mm; ND filter:

1%; hole: 400). Nuclear magnetic resonance glass tubes were used as support for the hydrogel samples for the Raman analysis.

Small angle scattering

Small angle X-ray scattering (SAXS) measurements were performed at the 12-ID-C,D beamline at the Advanced Photon Source at Argonne National Lab. 1D reductions were performed using beamline software and corrected for empty cell and solvent backgrounds. Hydrogel samples were swollen in ultrapure water, 50 or 100 mM sodium phosphate, pH = 7.6. Measurements of both hydrogels and films were performed at 25°C. Fitting of the scattering data was performed using software written in IGOR Pro made available by NIST.

RESULTS AND DISCUSSION

Design of Polypeptide-PEG Multiblocks by Macromolecular Polycondensation

Thiol-maleimide chemistry was used to produce linear alternating copolymers of ELP and PEG as illustrated by the scheme in Fig. 1c. Different reaction conditions, such as buffer type and pH , reaction time and ELP/PEG ratio, were tested in order to obtain copolymers with higher molecular weight. For instance, when ELP was used at lower molarity ratio than PEG, no residual ELP was detected. As it can be seen in Fig. 1d, PEG stained gels evidence that the higher molecular weight species result from coupling of PEG with ELP due to Michael addition since PEG presents a similar distribution pattern as the one found in the protein stained gel and both blocks have similar molar masses (ELP 25.9 kDa and PEG 20kDa). Based on the protein standards, an intense band accounted for PEG appears around 40 kDa . However, this result can be explained by the fact that PEG runs on the gel at a different apparent molar mass due to its electrophoretic mobility, that differs from the protein standard [42]. As expected for a polycondesation reaction, low molar mass species are always present. Densitometry analysis of SDS-PAGE was performed for multiple polypeptide and PEG stained gels, resulting on an average conjugation yield of 77.4% and 82.7% for ELP and PEG stained gels, respectively. The results also revealed that about 20% of low molar mass species are still present. The reaction yield was assumed to be around 80%, which are molecules with up to 8 blocks, and the molar masses are between 60 and 250 kDa , based on comparisons to protein standards.

a) MGWGSKCTSAGAGAGPEGRGDSTSGLVG[(IPAVGVPAVG)$_2$(IPAVG)]$_{10}$ ETTSRGDSAGAGAGPEGTSCKL

b)

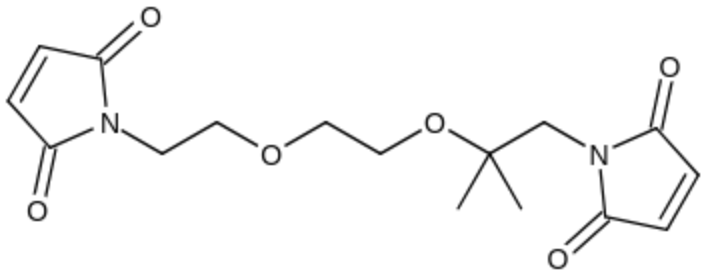

d)

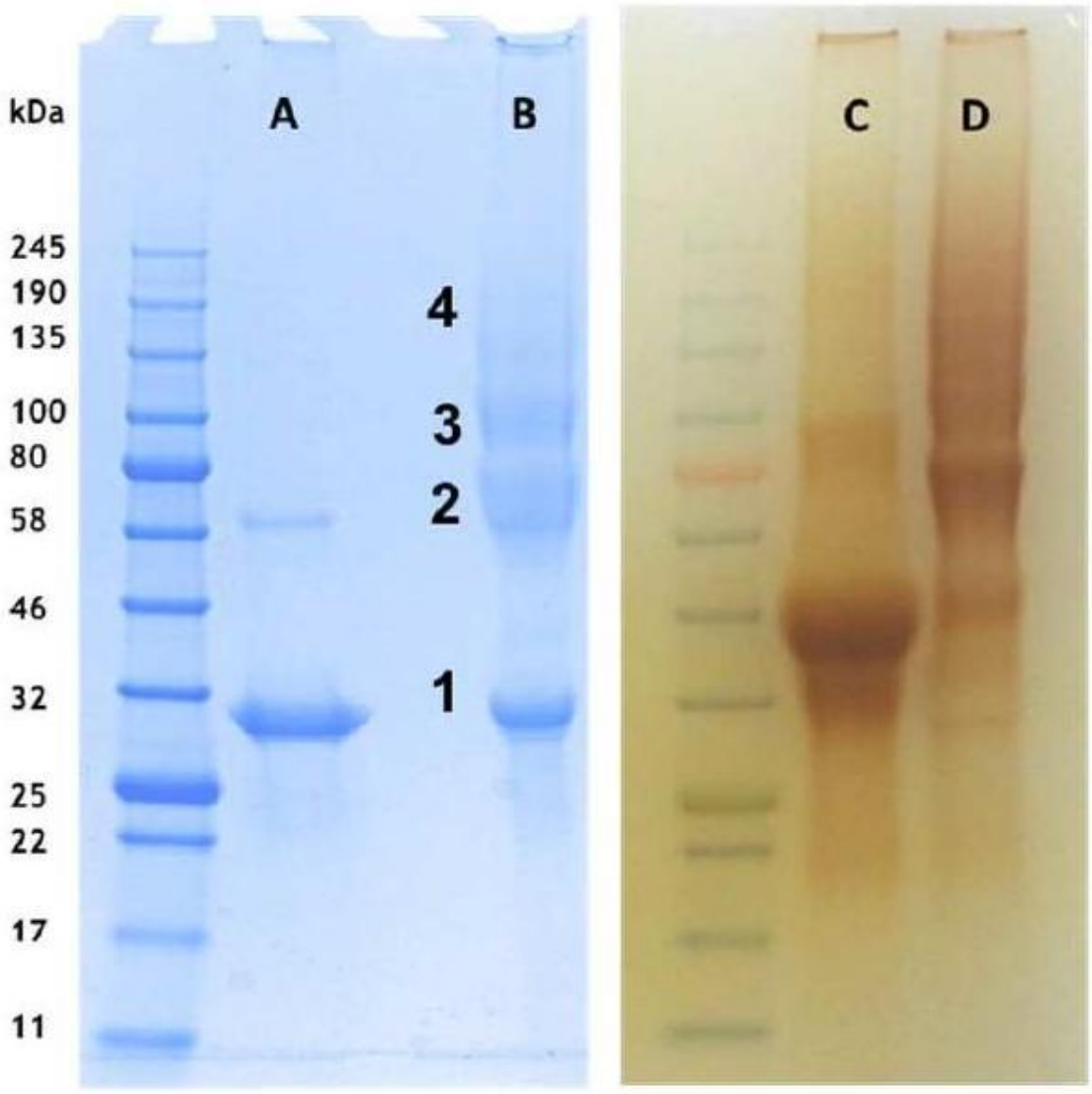

Figure 1 - Thiol-maleimide conjugation between ELP and PEG. a) Amino acid sequence of the elastin-like polypeptide; b) PEG structure; c) scheme of the thiol-maleimide reaction; d) analysis of the conjugation reaction by SDS-PAGE (lanes A and B: ELP and ELP/PEG

with gel stained for the protein, lanes C and D : PEG solution and ELP/PEG with gel stained for PEG); the numbers 2, 3 and 4 on lane *B* are associated to the formation of molecules with up to 8 blocks, respectively.

ELP and PEG have distinct thermal properties, therefore the copolymers formed present characteristics from both. DSC thermograms (Fig. 2a) show the typical PEG curve with a melting temperature of 68°C and degree of crystallinity of 77.6%. The first thermogram of lyophilized polypeptide presents a broad band between 60 and 140°C, likely due to the removal of bound water associated with the amino acid groups and absorbed water to the material between the time it was removed from the desiccator and loaded into the DSC. This endothermic band can also be related to thermally induced molecular rearrangement of ELP, which has been previously reported [43–44]. The lyophilized copolymer presents transitions of both individual blocks. The first endothermic peak is sharp and similar to the PEG melting peak, but shifted to lower temperatures (55°C). The degree of crystallinity calculated based on the theoretical amount of PEG in the conjugate also decreased to 54%. A lower melting point of the PEG block in the copolymer has been observed before in other PEG-peptide conjugates and may be related to hydrogen bonding between the amide group of the peptide and the ether linkage of the PEG segment [45]. The second endothermic peak, between 60 and 140°C, is similar to the one found for the peptide alone and should also be related to bound and absorbed water, as well as to thermally induced molecular rearrangement of the ELP.

According to TGA results, the copolymer loses water before 100°C and then degrades in two main steps over a range of 280 to 410°C similarly to the polypeptide alone (Fig. 2b). The first step, in the range of 280 to 340°C, corresponds to a 35% weight loss and is probably due to the ELP decomposition. The second degradation step, between 340 and 410°C, corresponds to a 55% weight loss and is associate to the degradation of the more stable portion of the polypeptide along with the PEG component. The residual 5% mass of ELP and ELP/PEG that appears at 500 °C is due to aromatic side chain amino acids, such as tryptophan. These species yield a char residue thermally stable at higher temperatures in nitrogen atmosphere [46].

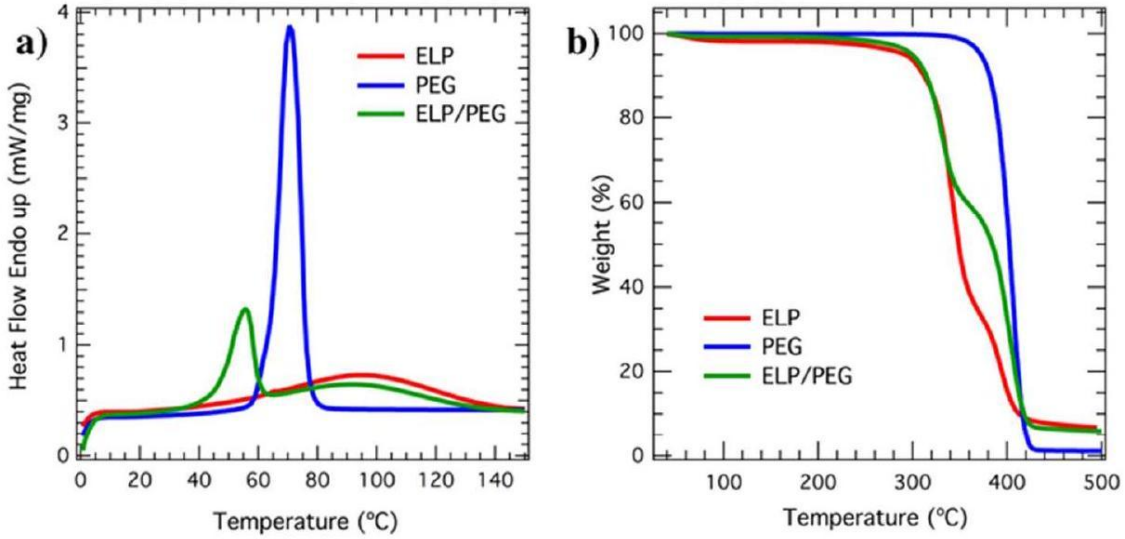

Figure 2 - Thermal properties of the initial polymers (ELP and PEG) and the copolymer formed (ELP/PEG) a) DSC and b) TGA heating ramps at 10 °C/min.

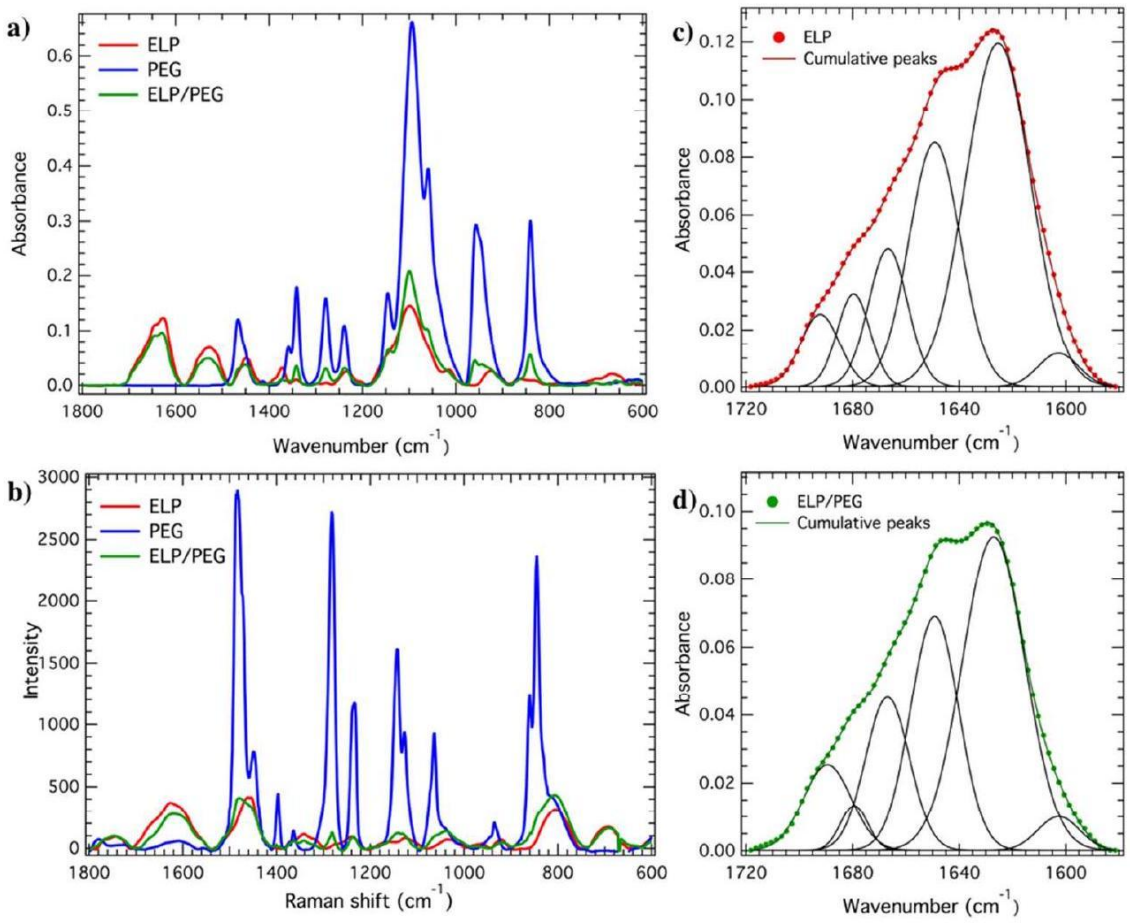

Figure 3 - Spectroscopic analysis of the polymers and copolymers formed. a) FTIR and b) Raman spectra of the polypeptide, PEG and copolymer; c) and d) deconvolution of the amide I band from FTIR spectra of ELP and ELP/PEG, respectively.

The overall chemical structure of the copolymer probed by FTIR and Raman spectroscopy is a combination of the structure of both ELP and PEG molecules. The FTIR spectrum for neat ELP (Fig. 3a) contains the characteristic peaks from the polypeptide repeat unit, which have been identified as follows: amide A at 3300 cm^{-1}($N-H$ stretching), amide I around 1650 cm^{-1}($C=O$ stretching), amide II at 1520 cm^{-1} (CN stretching and NH bending), amide III at 1230 cm^{-1} (CN stretching and NH bending) and amide IV at 660 cm^{-1} (OCN bending) [41,47]. PEG presents the typical bands already reported in the literature [48], and the copolymer has typical bands from both polypeptide and PEG, the presence of both polymers was also confirmed by Raman (Fig 3b).

The secondary structure of the copolymer, determined by analysis of the Amide I band in FTIR and Raman, showed similarities with ELP. The Amide I band of polypeptides and proteins has long been known to be sensitive to its secondary structure [49] and was studied to qualitatively compare ELP and ELP/PEG. Fig. 3c, d presents the deconvoluted spectra for both materials with the following peaks assigned: 1602 cm^{-1} (side chain contribution),

1625 cm^{-1} (β-sheet), 1649 cm^{-1} (random), 1666 cm^{-1} (turn), 1679 cm^{-1} (turn) and 1692 cm^{-1} (β-sheet) [41,49]. According to the peak areas calculated (Table 1), both lyophilized ELP and ELP/PEG present around 54%β sheet, 18% turn, 26% random coil and 3% side chain with no significant differences, evidencing that the conjugation with PEG does not substantially affect the ELP secondary structure. The high percentage of β-sheet and turns has been reported in the literature for a ELP with the sequence $(VPGVG)_n$ [50]. Raman studies of the amide I band also confirm the similarity between ELP and ELP/PEG structure and the major presence of β-sheet and turns that results from hydrogen bonding interactions between the repeating amino acid sequence, as previously reported [51].

Table 1 - Summary of the secondary structure percentage for the different samples calculated from the FTIR data of the Amide I band at room temperature.

Samples/Secondary Structure		α-helix (%)	β-sheet (%)	Turn (%)	Random coil (%)	Side chain (%)
Lyophilized	ELP	0	53 ± 1	18 ± 1	26 ± 1	3 ± 1
	ELP/PEG	0	54 ± 1	18 ± 1	25 ± 1	3 ± 1
Hydrogel	Water	0	51 ± 3	24 ± 3	24 ± 1	1 ± 1
	50 mM	0	54 ± 3	20 ± 3	25 ± 1	1 ± 1
	100 mM	0	51 ± 3	23 ± 3	24 ± 1	2 ± 1
Film	Water	0	55 ± 2	24 ± 2	19 ± 2	2 ± 1
	Water + P	0	54 ± 2	21 ± 2	23 ± 3	2 ± 1
	Buffer	0	54 ± 2	24 ± 2	20 ± 3	2 ± 1
	Buffer + P	0	52 ± 2	26 ± 3	20 ± 3	2 ± 1

Association of ELP Domains to Form Hydrogels

Hydrated ELP/PEG copolymer presented the same thermoresponsive property of ELP and formed a stiff hydrogel upon heating above its transition temperature (T_t) at a concentration of 15 wt%. When compared with the gelation of the polypeptide alone, as previously reported by Glassman et. al. [37], the ability to form a gel was not affected by the presence of PEG blocks.

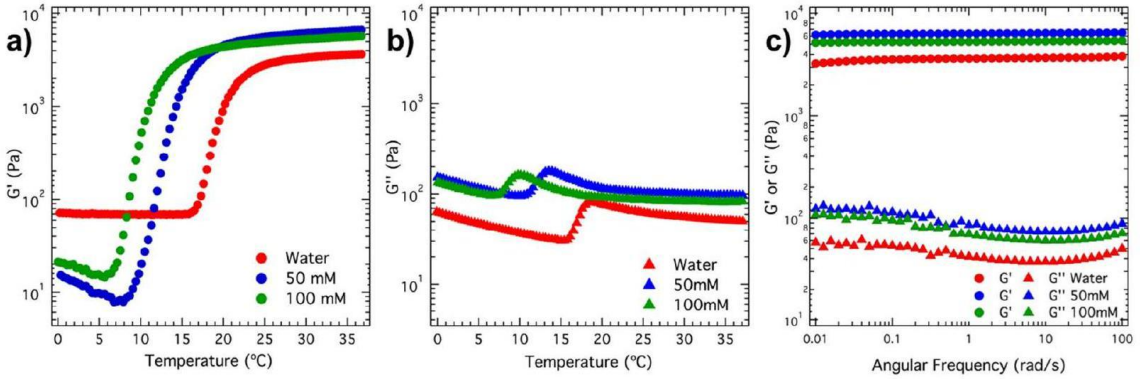

Figure 4 - Temperature sweep of the hydrogels dissolved in different solutions during heating cycles; a) and b) comparison of G' and G'' of the hydrogels; c) comparison of the frequency dependence of the viscoelastic moduli of the hydrogels at 37°C

As it can be seen in Fig. 4a and b, ELP/PEG hydrated in ultrapure water has G' similar to G'' at low temperatures, but the sample appears to be a viscous liquid when cold. The sharp increase of G' around 16°C corresponds to a stiffening transition and is caused by the folding and coacervation of ELPs, which act as physical crosslinker between the PEG chains [52]. Since there is no crossover of G' and G'', the T_t was estimated to be between 16 and 18°C. The hydrogels prepared in sodium phosphate buffer 50 or 100 mM (Fig 4b and c) have G' lower than G'', indicating that these materials are soften viscous liquids at low temperatures (below $6-8\,^{\circ}C$), which can be explained by a kinect effect. Above these temperatures, the presence of salt changes the T_t from 16°C (in water) to 12°C and 9°C (for 50 and 100 mM , respectively) and makes the gels stronger. The presence of salt increases the ionic strength of a solution and it drives the ELP chains to precipitate at lower temperatures [17, 53]. The hydrogels were also subjected to cooling cycles that showed reversibility of the copolymer network formed (SI3). The hysteresis in the network disassembly upon cooling is consistent with solvation hysteresis typically observed for ELPs with alanine in the third position of the repeat pentapeptide [54].

Frequency sweeps at 37 °C reveal the same behavior in all hydrogel samples (Fig 4c), G' is larger than G'', and both are frequency independent across the experimental range, further confirming that an elastic solid like network was formed. DSC thermograms of these materials also show a small endothermic peak that corresponds to the formation of the hydrogel (Table 2) and the transition temperatures calculated from DSC and from the rheological measurements are similar. Pure ELP hydrogels prepared in water at 15wt% present a T_t of 19 °C[37], which is just slightly higher than the T_t found for the copolymer. One can conclude that the presence of PEG blocks has less influence on the temperature of the gelation transition than the addition of salt.

Table 2 - Comparison between the transition temperature obtained from rheology and DSC.

	Rheology (°C)	DSC (°C)
Water	16 – 18	17
50 mM	12	12
100 mM	9	9

The Amide I band from FTIR spectra of the hydrogels was analyzed to evaluate possible changes in the copolymer secondary structure after gelation. Fig. 5 presents the deconvoluted spectra with the following peaks assigned: 1627 cm^{-1} (β-sheet), 1646 cm^{-1} (random), 1662 cm^{-1} (turn), 1677 cm^{-1} (turn) and 1695 cm^{-1} (β-sheet) [41,49]. According to the peak areas calculated, ELP/PEG hydrogels have $51 \pm 3\%\beta$-sheet, $23 \pm 3\%$ turn and $25 \pm 1\%$ random coil. Above the T_t, all samples appear to have a similar secondary structure to the lyophilized material (Table 1). These results suggest that the ELP component of the networks sustain the same structure independent of the salt concentration used to form the hydrogels.

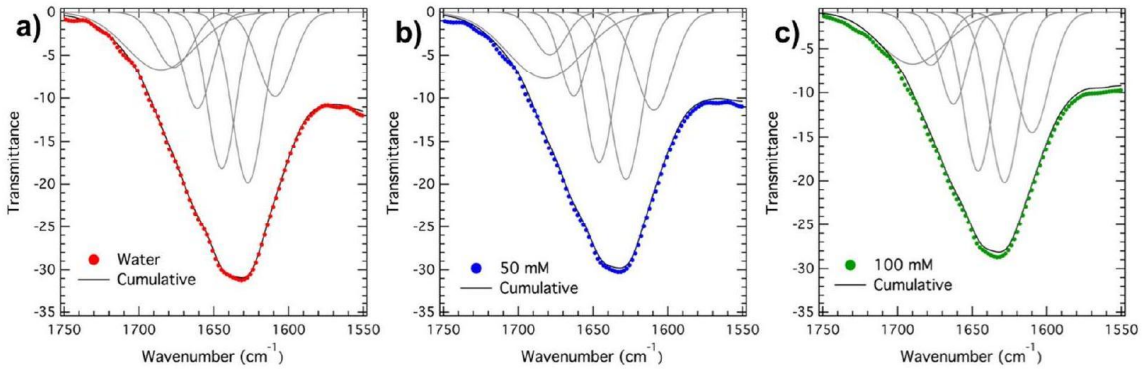

Figure 5 - Deconvolution of the amide I band from FTIR spectra, at room temperature, of the ELP/PEG hydrogels prepared with different solutions: a) water, b) 50 mM and c) 100 mM sodium phosphate buffer.

Fig. 6 shows small-angle x-ray scattering (SAXS) results taken on the hydrogels. The best fit was achieved using the fuzzy sphere model described by the following equation for intensity [55] :

$$I(q) = \frac{(\Delta\rho)^2\varphi}{\langle V_{\text{particle}} \rangle} P(q)S(q) + \frac{I_{\text{lor}}}{1+\xi^2 q^2} + B \qquad (eq.2)$$

where φ is the volume fraction of the spheres, $\langle V_{\text{particle}} \rangle$ is the average sphere volume, $\Delta\rho$ is the difference in scattering length density between the solvent and the sphere, I_{lor} is the Lorentz scale and ξ is the fluctuation correlation length (which are related to mesh size in the network), B is the background, P(q) is the form factor given by

$$P(q) = \frac{3[\sin(qR) - qR\cos(qr)]}{(qR)^3} e^{\left(\frac{-(\sigma_{\text{surf}}\, q)^2}{2}\right)} \qquad (eq.3)$$

where σ_{surf} is the width of the smeared particle surface. S(q) is the structure factor that accounts for interparticle interactions, and it was calculated by solving the Ornstein-Zernike (OZ) equation using the Two-Yukawa potential [55–56] :

$$\frac{V(r)}{k_B T} = \begin{cases} \infty, (0 < r < 1) & (eq.4) \\ -K_1 \frac{e^{-Z_1(r-1)}}{r} - K_2 \frac{e^{-Z_2(r-1)}}{r}, (r > 1) & (eq.4) \end{cases}$$

and the mean spherical approximation (MSA) closure:

$$\begin{cases} h(r) = -1, (0 < r < 1) & (eq.5) \\ c(r) = -\frac{V(r)}{k_B T} = -K_1 \frac{e^{-Z_1(r-1)}}{r} + K_2 \frac{e^{-Z_2(r-1)}}{r}, (r > 1) & (eq.5) \end{cases}$$

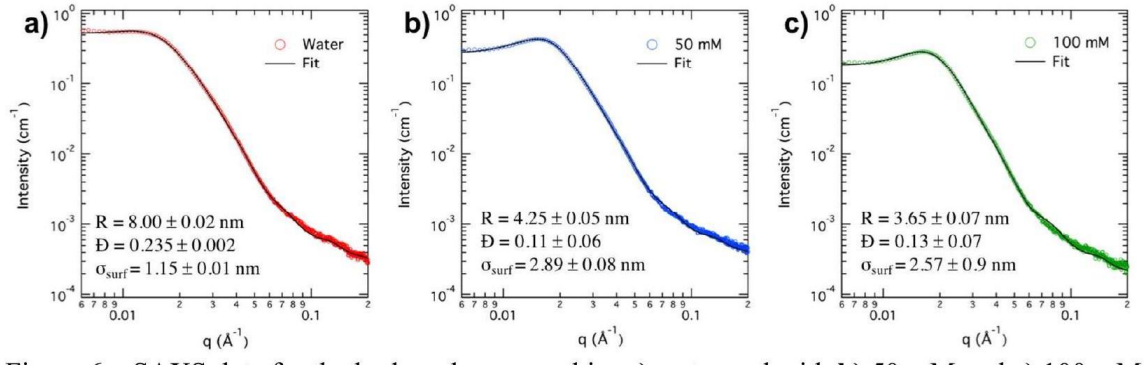

Figure 6 - SAXS data for the hydrogels prepared in: a) water and with b) 50 mM and c) 100 mM buffer solution. The curves are fit by the fuzzy sphere model, where R is the sphere radius, Đ is the sphere dispersity, and σ_{surf} is the interface thickness of the fuzzy spheres.

The data fitting using the fuzzy sphere model clearly shows the formation of a network composed essentially by ELP sphere-like aggregates (when above its T_t) surrounded by PEG most likely in the "fuzzy" interface. The hydrogel prepared in water has nanoscale spherical building blocks with an average radius of 8.0 nm and an interface thickness of 1.15 nm , while the hydrogels prepared in 50 mM and 100 mM buffer have radii of 4.25 and 3.65 nm , and interface thickness of 2.89 and 2.57 nm , respectively. The model predictions show that the type of solution used to form the hydrogels does not strongly affect the structure of the building blocks of the network, instead influences its mean radius and interface thickness. Overall, the increase in salt concentration leads to a decrease of the average cluster size (from 9.15 nm for water, 7.14 nm for 50 mM , to 6.22 nm for 100 mM), which suggests the formation of more compact spheres and/or less water arrested in the ELP core. Also, the network correlation length is lower for the hydrogels prepared with salt (16.7 nm for 50 mM and 20.6 nm for 100 mM), indicating of a more compact network, when compared to the hydrogels prepared in water (22.3 nm). The higher radius and smaller interface for the water hydrogel may explain the higher T_t and slightly lower G' found in rheology data. According to the assembly model proposed for the hydrogels, the RGD peptides on the ELP are probably on the core of the spheres,

particularly for the residual protein, and close to or in the fuzzy interface when the ELP is conjugated to PEG.

The use of self-assembling multiblock copolymers provides a useful new strategy for the preparation of ELP hydrogels. Often, ELP physical hydrogels have been reported to be mechanically weak [57–58], while cross-linked ELP hydrogels display improved mechanical properties [22]. The ELP-PEG block copolymer produced in this work is able to form reversible physical hydrogels, even with the incorporation of PEG blocks, together with high modulus without use of crosslinking agents. The use of the multiblock synthesis strategy also eliminates the use of excess polymer traditionally required to drive conversion, which makes this strategy scalable for the production of gels. Also, the ELP used contains two cell-adhesive RGD peptides near the N - and C termini that make these hydrogels interesting for biomedical applications.

Association of ELP Domains to Form Films

Protein films have attracted a great deal of interest [59], including for artificial extracellular matrix (aECM) films prepared with ELP sequences and also different crosslinking agents [60–61]. Therefore, thin films of ELP/PEG copolymer were prepared using different solutions and with or without addition of a plasticizer and presented different mechanical properties.

Dynamic mechanical analysis (DMA) studies were performed, and Fig. 7 a) shows the experimental data for E'. In general, as expected, the addition of plasticizer decreases E' of the samples, but samples where the copolymer was dissolved in buffer, exhibit a smaller decrease of

E' with the addition of plasticizer when compared with the samples dissolved in just water. It is clear that all samples have qualitatively similar behavior along the temperature, exhibiting a decrease in E' around 50 °C associated to a softening transition of the material. This is consistent with the endothermic peak in the DSC results (Fig 7 b) that may be related to an increase in deformability of the PEG chains. Even though there were not noticed changes on the DSC peak temperature, the addition of plasticizer slightly changes the temperature where E' starts to decrease from 38 to 34°C, in films prepared in water and from 46 to 40°C, in films prepared in buffer.

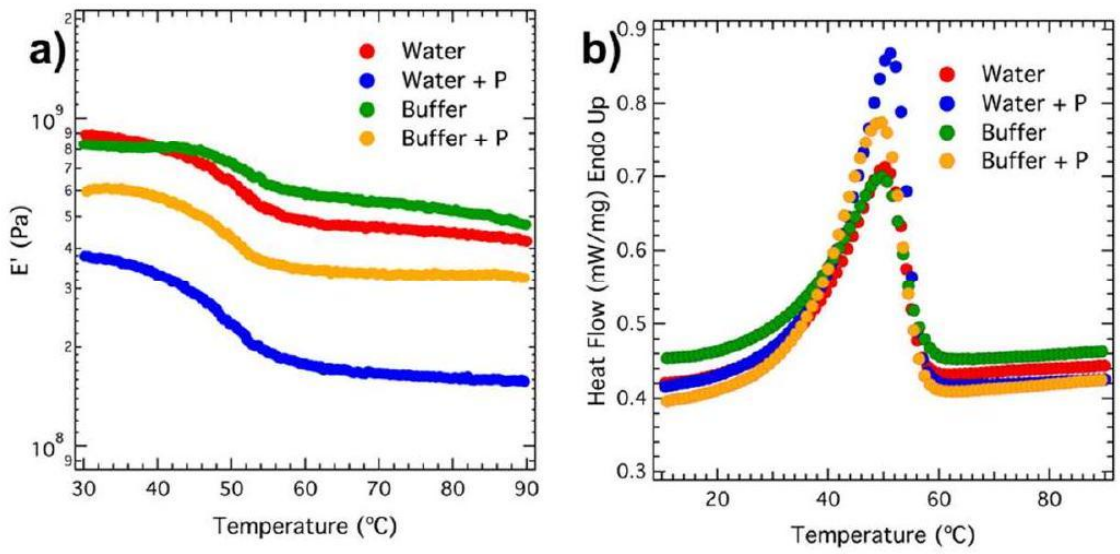

Figure 7 - DMA results of a) Elastic Storage Modulus E') and b) DSC thermogram of the different films prepared.

Fig. 8 presents the deconvoluted FTIR spectra for the films with the following peaks assigned: 1603 cm^{-1} (side chain contribution), 1627 cm^{-1} (β-sheet), 1648 cm^{-1} (random), 1665 cm^{-1} (turn), 1679 cm^{-1} (turn) and 1689 cm^{-1}(β-sheet)[41]. According to the peak areas calculated, ELP/PEG films have an average of $54 \pm 2\%\beta$-sheet, $24 \pm 2\%$ turn, $20 \pm 3\%$ random coil and $2 \pm 0.4\%$ side chain. The small differences between the calculated percentages are within the experimental error, suggesting that ELP presents the same secondary structure in all films. These results are also in accordance with the RAMAN experiments performed (SI).

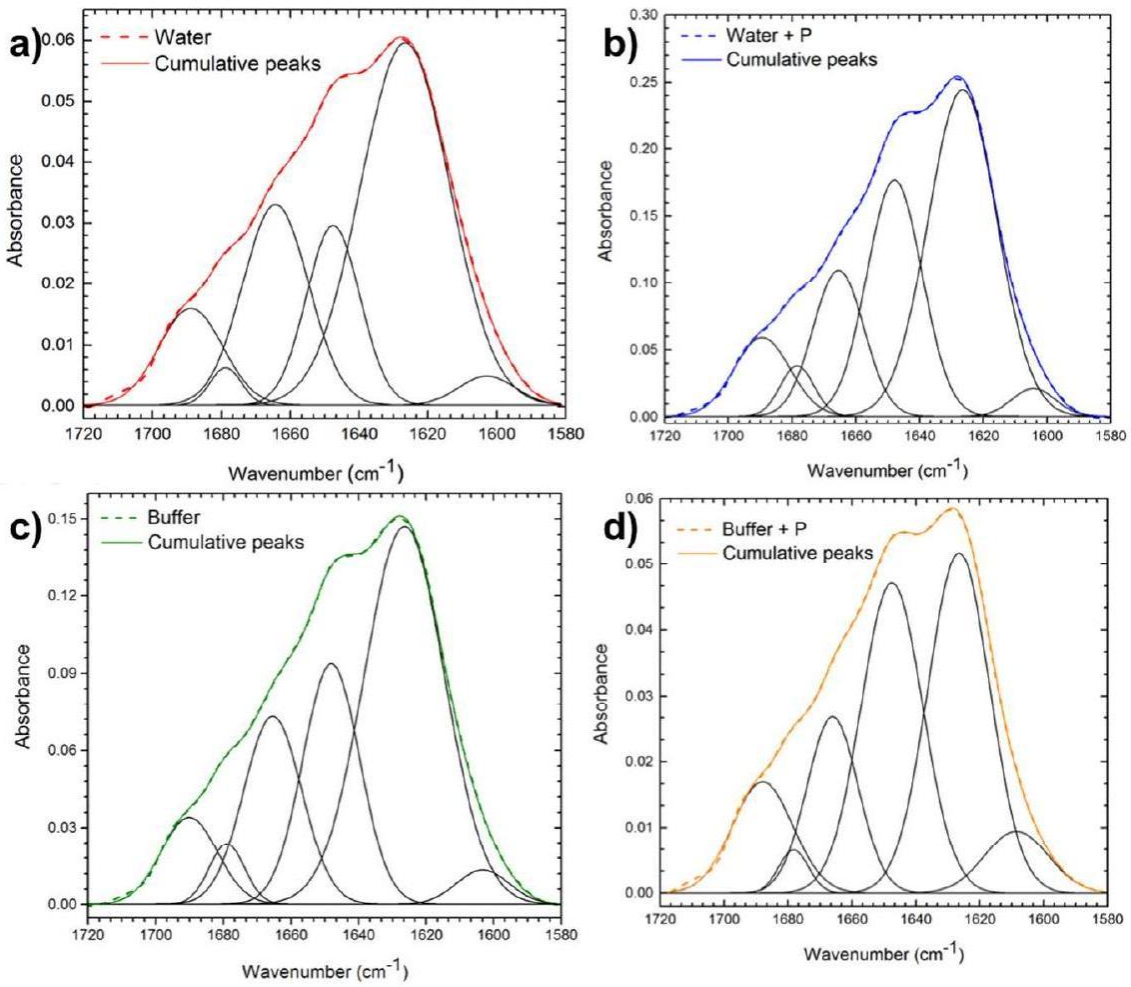

Figure 8 - Deconvolution of the amide I band from FTIR spectra of the ELP/PEG films prepared with a) water, b) water with plasticizer, c) 50 mM buffer and d) buffer with plasticizer.

Structure characterization of the thin films suggests that they have a structure of aggregated spherical particles, consistent with what would be expected for formation of ELP physical crosslink domains followed by drying of the material. The best fits of small-angle x-ray scattering (SAXS) results (Fig. 9) were obtained with a fractal poly sphere model described by the following equation for intensity [62] :

$$I(q) = P(q)S(q) + B \qquad (eq.6)$$

$$P(q) = \varphi \frac{4\pi}{3} R_0 (\Delta\rho)^2 F(qR_0)^2 \qquad (eq.7)$$

where P(q) is the scattering from randomly distributed spherical building block particles having radius R_0, scattering length density $\Delta\rho$ and polydispersity of the sphere radius is described by Schulz distribution:

$$F(R) = (z+1)^{z+1} x^z \frac{\exp\left[-(z+1)x\right]}{R_{\text{avg}}\,\Gamma(z+1)} \qquad (eq.8)$$

where R_{avg} is the mean radius, $x = R/R_{avg}$, z is related to the polydispersity, $p = \sigma/$ Ravg, by $z = 1/\mathrm{p}2 - 1, \sigma 2$ is the variance of the distribution.

The spherical building blocks aggregate to form fractal-like clusters. The clusters have a correlation length ξ, corresponding to their overall size, and self-similarity dimension D_f. The interference from building blocks of the fractal-like cluster was calculated from:

$$S(q) = 1 + \frac{\sin\left[(D_f - 1)\tan^{-1}(q\xi)\right] D_f \Gamma(D_f - 1)}{(qR_0)^D f_{[1+1/(q^2\xi^2)]}}^{(Df^{-1})/2} \qquad (eq. 9)$$

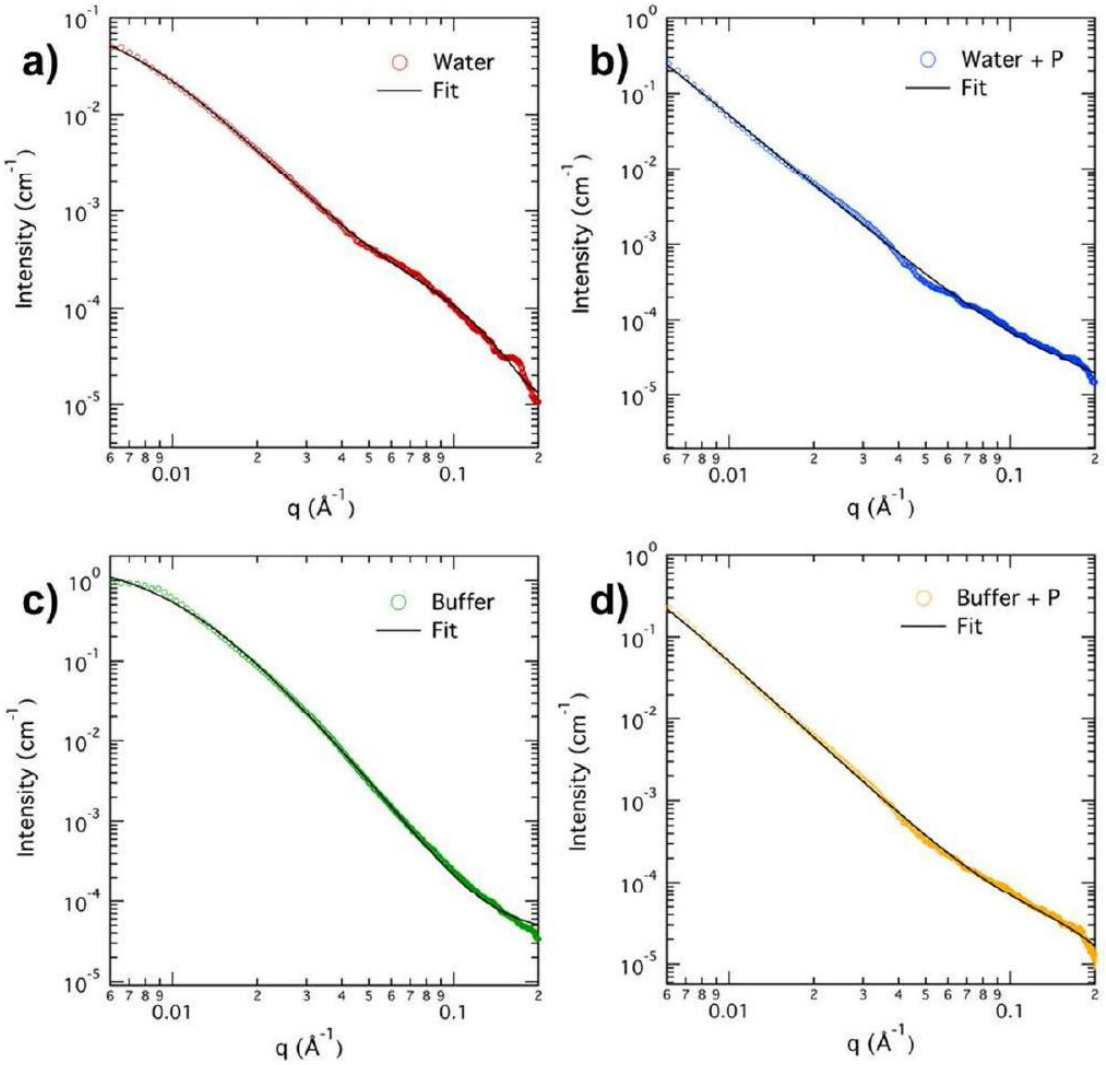

Figure 9 - SAXS data for the films a) water, b) water + plasticizer, c) buffer and d) buffer + plasticizer, with the curves fitted by the fractal poly sphere model.

The fit of the data using the fractal poly sphere model evidences that the ELP/PEG copolymer forms spherical fractal-like clusters, probably with the ELP aggregated in the centre and surrounded by the PEG chains. The results presented in Table 3 show changes in the mean radius

of the films, being higher for films without plasticizer, and slightly lower for films prepared in buffer, as it was previously observed for the hydrogels. It is also visible that films with the addition of plasticizer have an overall bigger size than the samples without it, since the correlation length changes from 12.4 to 25.8 nm in the case of films prepared in water, and from 10.5 to 26.7 nm for films prepared in buffer. This suggests that the plasticizer may be located in the PEG chains around the ELP aggregates, increasing the distance between ELP domains. The model predictions show that the addition of plasticizer and the use of different solutions to prepare the films did not affect the assembly of the building blocks, but had some influence on the size of the clusters. This is also in accordance with the differences in E' observed in the DMA results, since bigger and less compact clusters tend to be more flexible and with lower E' values. Localization of the plasticizer in amorphous PEG regions is also consistent with the smaller radius from the SAXS fits.

Table 3 - Table of the SAXS fit by the fractal poly sphere model, where R is the sphere radius, Đ is the sphere dispersity, D_f the fractal dimension and ξ the correlation length.

	Water	Water + P	Buffer	Buffer + P
R (nm)	2.49 ± 0.01	1.97 ± 0.01	2.09 ± 0.01	1.60 ± 0.01
Đ	0.10 ± 0.01	0.10 ± 0.01	0.10 ± 0.04	0.100 ± 0.01
D_f	2.71 ± 0.01	2.75 ± 0.02	2.9 ± 0.1	2.81 ± 0.02
ξ(nm)	12.4 ± 0.1	25.8 ± 0.4	10.5 ± 0.1	26.7 ± 0.4

Using a simple technique of solution-casting, the ELP-PEG block copolymer here developed enables the formation of transparent thin films without use of organic solvents. The properties of the copolymer films, including the possible production without additives and plasticizers, and the presence of the RGD motif, make these films interesting for biomedical applications in the form of thin coatings that could promote cell-adhesion.

CONCLUSIONS

Thiol maleimide chemistry was successfully used to produce linear alternating multi-blocks of ELP and PEG by macromolecular coupling in solution. This new strategy enables scalable synthesis of multiblock copolymers using stoichiometric PEG and ELP, different than most other bioconjugate reactions which are driven by excess polymer. One of the most important features of the material is that the hydrated copolymer preserved the thermoresponsive properties from the ELP block and formed physical hydrogels at 15wt% with different transition temperatures that can be tuned based on salt concentration. Previously, ELP-PEG networks were formed as chemical crosslinked networks. The copolymer was also processed in the form of transparent thin films with variation of salt concentration and addition of 5% plasticizer that influenced the materials' properties. Small angle scattering indicates that the copolymer hydrogels form a network with sphere-like aggregates and a "fuzzy" interface, while the films form a fractal network of nanoscale aggregates. The biocompatible nature of the polypeptides and PEG may make these copolymers potentially useful for biomedical applications.

ACKNOWLEDGMENT

This research was supported by the MIT Portugal Program. SAXS measurements were performed at the 12-ID-C,D beamline at the Advanced Photon Source at Argonne National Lab, supported by the National Science Foundation.

REFERENCES

1. Wegst, U. G. K.; Ashby, M. F., The mechanical efficiency of natural materials. Philos. Mag. 2004, 84 (21), 2167-2186.
2. Johnson, J. C.; Wanasekara, N. D.; Korley, L. T., Utilizing peptidic ordering in the design of hierarchical polyurethane/ureas. Biomacromolecules 2012, 13 (5), 1279-1286.
3. Olsen, B. D., Engineering materials from proteins. AIChE J. 2013, 59 (10), 3558-3568.
4. Wegst, U. G.; Bai, H.; Saiz, E.; Tomsia, A. P.; Ritchie, R. O., Bioinspired structural materials. Nat. Mater. 2015, 14 (1), 23-36.
5. Schlaad, H.; Diehl, C.; Gress, A.; Meyer, M.; Demirel, A. L.; Nur, Y.; Bertin, A., Poly(2oxazoline)s as Smart Bioinspired Polymers. Macromol. Rapid Commun. 2010, 31 (6), 511-525.
6. Wang, Q.; Yang, Z.; Zhang, X.; Xiao, X.; Chang, C. K.; Xu, B., A Supramolecular-Hydrogel-Encapsulated Hemin as an Artificial Enzyme to Mimic Peroxidase. Angew. Chem., Int. Ed. 2007, 46 (23), 4285-4289.
7. Badrossamay, M. R.; Balachandran, K.; Capulli, A. K.; Golecki, H. M.; Agarwal, A.; Goss, J. A.; Kim, H.; Shin, K.; Parker, K. K., Engineering hybrid polymer-protein super-aligned nanofibers via rotary jet spinning. Biomaterials 2014, 35 (10), 3188-3197.
8. Lin, C.-Y.; Liu, J. C., Modular protein domains: an engineering approach toward functional biomaterials. Curr. Opin. Biotechnol. 2016, 40, 56-63.
9. Obermeyer, A. C.; Olsen, B. D., Synthesis and application of protein-containing block copolymers. ACS Macro Lett. 2015, 4 (1), 101-110.
10. Hume, J.; Sun, J.; Jacquet, R.; Renfrew, P. D.; Martin, J. A.; Bonneau, R.; Gilchrist, M. L.; Montclare, J. K., Engineered coiled-coil protein microfibers. Biomacromolecules 2014, 15 (10), 3503-3510.
11. Meyers, M. A.; Chen, P.-Y.; Lin, A. Y.-M.; Seki, Y., Biological materials: Structure and mechanical properties. Prog. Mater. Sci. 2008, 53 (1), 1-206.
12. White, J. D.; Wilker, J. J., Underwater bonding with charged polymer mimics of marine mussel adhesive proteins. Macromolecules 2011, 44 (13), 5085-5088.
13. Collini, E.; Wong, C. Y.; Wilk, K. E.; Curmi, P. M.; Brumer, P.; Scholes, G. D., Coherently wired light-harvesting in photosynthetic marine algae at ambient temperature. Nature 2010, 463 (7281), 644.
14. Riva, S., Laccases: blue enzymes for green chemistry. Trends Biotechnol. 2006, 24 (5), 219-226.

15. Chen, P.; He, C., A general strategy to convert the MerR family proteins into highly sensitive and selective fluorescent biosensors for metal ions. J. Am. Chem. Soc. 2004, 126 (3), 728-729.

16. Urry, D.; Long, M.; Cox, B.; Ohnishi, T.; Mitchell, L.; Jacobs, M., The synthetic polypentapeptide of elastin coacervates and forms filamentous aggregates. Biochim. Biophys. Acta, Protein Struct. 1974, 371 (2), 597-602.

17. Bellingham, C. M.; Woodhouse, K. A.; Robson, P.; Rothstein, S. J.; Keeley, F. W., Selfaggregation characteristics of recombinantly expressed human elastin polypeptides. Biochim. Biophys. Acta, Protein Struct. Mol. Enzymol. 2001, 1550 (1), 6-19.

18. Meyer, D. E.; Chilkoti, A., Genetically encoded synthesis of protein-based polymers with precisely specified molecular weight and sequence by recursive directional ligation: examples from the elastin-like polypeptide system. Biomacromolecules 2002, 3 (2), 357-367.

19. Krishna, U. M.; Martinez, A. W.; Caves, J. M.; Chaikof, E. L., Hydrazone selfcrosslinking of multiphase elastin-like block copolymer networks. Acta Biomater. 2012, 8 (3), 988-997.

20. Betre, H.; Ong, S. R.; Guilak, F.; Chilkoti, A.; Fermor, B.; Setton, L. A., Chondrocytic differentiation of human adipose-derived adult stem cells in elastin-like polypeptide. Biomaterials 2006, 27 (1), 91-99.

21. Nuhn, H.; Klok, H.-A., Secondary structure formation and LCST behavior of short elastin-like peptides. Biomacromolecules 2008, 9 (10), 2755-2763.

22. Trabbic-Carlson, K.; Setton, L. A.; Chilkoti, A., Swelling and mechanical behaviors of chemically cross-linked hydrogels of elastin-like polypeptides. Biomacromolecules 2003, 4 (3), 572-580.

23. Lim, D. W.; Nettles, D. L.; Setton, L. A.; Chilkoti, A., In situ cross-linking of elastin-like polypeptide block copolymers for tissue repair. Biomacromolecules 2008, 9 (1), 222.

24. Daamen, W. F.; Veerkamp, J.; Van Hest, J.; Van Kuppevelt, T., Elastin as a biomaterial for tissue engineering. Biomaterials 2007, 28 (30), 4378-4398.

25. Krishna, O. D.; Kiick, K. L., Protein-and peptide-modified synthetic polymeric biomaterials. Pept. Sci. 2010, 94 (1), 32-48.

26. Shu, J. Y.; Panganiban, B.; Xu, T., Peptide-polymer conjugates: From fundamental science to application. Annu. Rev Phys. Chem. 2013, 64, 631-657.

27. Pelegri-O'Day, E. M.; Lin, E.-W.; Maynard, H. D., Therapeutic protein-polymer conjugates: advancing beyond PEGylation. J. Am. Chem. Soc. 2014, 136 (41), 14323-14332.

28. Cobo, I.; Li, M.; Sumerlin, B. S.; Perrier, S., Smart hybrid materials by conjugation of responsive polymers to biomacromolecules. Nat. Mater. 2015, 14 (2), 143-159.

29. Pechar, M.; Brus, J.; Kostka, L.; Koňák, Č.; Urbanová, M.; Šlouf, M., Thermoresponsive Self-Assembly of Short Elastin-Like Polypentapeptides and Their Poly (ethylene glycol) Derivatives. Macromol. Biosci. 2007, 7 (1), 56-69.

30. Ayres, L.; Vos, M. R.; Adams, P. H. M.; Shklyarevskiy, I. O.; van Hest, J. C., Elastinbased side-chain polymers synthesized by ATRP. Macromolecules 2003, 36 (16), 5967-5973.

31. Rathore, O.; Sogah, D. Y., Self-assembly of β-sheets into nanostructures by poly (alanine) segments incorporated in multiblock copolymers inspired by spider silk. J. Am. Chem. Soc. 2001, 123 (22), 5231-5239.

32. Grieshaber, S. E.; Farran, A. J.; Lin-Gibson, S.; Kiick, K. L.; Jia, X., Synthesis and Characterization of Elastin- Mimetic Hybrid Polymers with Multiblock, Alternating Molecular Architecture and Elastomeric Properties. Macromolecules 2009, 42 (7), 2532-2541.

33. Sahin, E.; Kiick, K. L., Macromolecule-induced assembly of coiled-coils in alternating multiblock polymers. Biomacromolecules 2009, 10 (10), 2740-2749.

34. Miller, J. S.; Shen, C. J.; Legant, W. R.; Baranski, J. D.; Blakely, B. L.; Chen, C. S., Bioactive hydrogels made from step-growth derived PEG-peptide macromers. Biomaterials 2010, 31 (13), 3736-3743.

35. Grieshaber, S. E.; Farran, A. J.; Bai, S.; Kiick, K. L.; Jia, X., Tuning the properties of elastin mimetic hybrid copolymers via a modular polymerization method. Biomacromolecules 2012, 13 (6), 1774-1786.

36. Glassman, M. J.; Olsen, B. D., Arrested phase separation of elastin-like polypeptide solutions yields stiff, thermoresponsive gels. Biomacromolecules 2015, 16 (12), 3762-3773.

37. Glassman, M. J.; Avery, R. K.; Khademhosseini, A.; Olsen, B. D., Toughening of Thermoresponsive Arrested Networks of Elastin-Like Polypeptides To Engineer Cytocompatible Tissue Scaffolds. Biomacromolecules 2016, 17 (2), 415-426.

38. Nair, D. P.; Podgórski, M.; Chatani, S.; Gong, T.; Xi, W.; Fenoli, C. R.; Bowman, C. N., The thiol-Michael addition click reaction: a powerful and widely used tool in materials chemistry. Chem. Mater. 2013, 26 (1), 724-744.

39. Pielichowski, K.; Flejtuch, K., Differential scanning calorimetry studies on poly (ethylene glycol) with different molecular weights for thermal energy storage materials. Polym. Adv. Technol. 2002, 13 (10-12), 690-696.

40. Martín, L.; Arias, F. J.; Alonso, M.; García-Arévalo, C.; Rodríguez-Cabello, J. C., Rapid micropatterning by temperature-triggered reversible gelation of a recombinant smart elastin-like tetrablock-copolymer. Soft Matter 2010, 6 (6), 1121-1124.

41. Yang, H.; Yang, S.; Kong, J.; Dong, A.; Yu, S., Obtaining information about protein secondary structures in aqueous solution using Fourier transform IR spectroscopy. Nat. Protoc. 2015, 10 (3), 382-396.

42. Dhara, D.; Chatterji, P. R., Electrophoretic transport of poly (ethylene glycol) chains through poly (acrylamide) gel. The Journal of Physical Chemistry B 1999, 103 (40), 8458-8461.

43. Amruthwar, S. S.; Puckett, A. D.; Janorkar, A. V., Preparation and characterization of novel elastin-like polypeptide-collagen composites. J. Biomeb. Mater. Res., Part A 2013, 101 (8), 2383-2391.

44. Rodriguez-Cabello, J.; Alonso, M.; Diez, M.; Caballero, M.; Herguedas, M., Structural investigation of the poly (pentapeptide) of elastin, poly (GVGVP), in the solid state. Macromol. Chem. Phys. 1999, 200 (8), 1831-1838.

45. Castelletto, V.; Newby, G.; Zhu, Z.; Hamley, I.; Noirez, L., Self-assembly of PEGylated peptide conjugates containing a modified amyloid β-peptide fragment. Langmuir 2010, 26 (12), 9986-9996.

46. Mallakpour, S.; Rafiee, Z., Use of ionic liquid and microwave irradiation as a convenient, rapid and eco-friendly method for synthesis of novel optically active and thermally stable aromatic polyamides containing N-phthaloyl-l-alanine pendent group. Polym. Degrad. Stab. 2008, 93 (4), 753-759.

47. Kong, J.; Yu, S., Fourier transform infrared spectroscopic analysis of protein secondary structures. Acta Biochim. Biophys. Sin. 2007, 39 (8), 549-559.

48. Shameli, K.; Bin Ahmad, M.; Jazayeri, S. D.; Sedaghat, S.; Shabanzadeh, P.; Jahangirian, H.; Mahdavi, M.; Abdollahi, Y., Synthesis and characterization of polyethylene glycol mediated silver nanoparticles by the green method. Int. J. Mol. Sci. 2012, 13 (6), 6639-6650.

49. Barth, A., Infrared spectroscopy of proteins. Biochim. Biophys. Acta, Bioenerg. 2007, 1767 (9), 1073-1101.

50. Serrano, V.; Liu, W.; Franzen, S., An Infrared Spectroscopic Study of the Conformational Transition of Elastin-Like Polypeptides. Biophys. J. 2007, 93 (7), 2429-2435.

51. Kim, W.; Chaikof, E. L., Recombinant elastin-mimetic biomaterials: emerging applications in medicine. Adv. Drug Delivery Rev. 2010, 62 (15), 1468-1478.

52. Cheng, J.; Park, M.; Hyun, J., Thermoresponsive hybrid hydrogel of oxidized nanocellulose using a polypeptide crosslinker. Cellulose 2014, 21 (3), 1699-1708.

53. Fong, B. A.; Wu, W.-Y.; Wood, D. W., Optimization of ELP-intein mediated protein purification by salt substitution. Protein Expression Purif. 2009, 66 (2), 198-202.

54. Wright, E. R.; Conticello, V. P., Self-assembly of block copolymers derived from elastinmimetic polypeptide sequences. Adv. Drug Delivery Rev. 2002, 54 (8), 1057-1073.

55. Kline, S. R., Reduction and analysis of SANS and USANS data using IGOR Pro. J. Appl. Crystallogr. 2006, 39 (6), 895-900.

56. Broccio, M.; Costa, D.; Liu, Y.; Chen, S.-H., The structural properties of a two-Yukawa fluid: Simulation and analytical results. J. Chem. Phys. 2006, 124 (8), 084501.

57. Yan, C.; Pochan, D. J., Rheological properties of peptide-based hydrogels for biomedical and other applications. Chem. Soc. Rev. 2010, 39 (9), 3528-3540.

58. Asai, D.; Xu, D.; Liu, W.; Quiroz, F. G.; Callahan, D. J.; Zalutsky, M. R.; Craig, S. L.; Chilkoti, A., Protein polymer hydrogels by in situ, rapid and reversible self-gelation. Biomaterials 2012, 33 (21), 5451-5458.

59. Costa, R. R.; Custódio, C. A.; Testera, A. M.; Arias, F. J.; Rodríguez-Cabello, J. C.; Alves, N. M.; Mano, J. F., Stimuli-responsive thin coatings using elastin-like polymers for biomedical applications. Adv. Func. Mater. 2009, 19 (20), 3210-3218.

60. Liu, J. C.; Tirrell, D. A., Cell response to RGD density in cross-linked artificial extracellular matrix protein films. Biomacromolecules 2008, 9 (11), 2984-2988.

61. Nowatzki, P. J.; Tirrell, D. A., Physical properties of artificial extracellular matrix protein films prepared by isocyanate crosslinking. Biomaterials 2004, 25 (7), 1261-1267.

62. Şen, E. H.; Ide, S.; Bayari, S. H.; Hill, M., Micro-and nano-structural characterization of six marine sponges of the class Demospongiae. Eur. Biophys. J. 2016, 45 (8), 831-842.